Coherence during Scattering of Fast H Atoms from a LiF(001) Surface

J. Lienemann, A. Schüller, D. Blauth, J. Seifert, S. Wethekam, M. Busch, K. Maass, and H. Winter*

Institut für Physik, Humboldt Universität zu Berlin, Brook-Taylor-Straße 6, D-12489 Berlin-Adlershof, Germany
(Received 26 September 2010; published 11 February 2011)

The coherence for diffraction effects during grazing scattering of fast hydrogen and helium atoms from a LiF(001) surface with energies up to some keV is investigated via the coincident detection of two-dimensional angular distributions for scattered projectiles with their energy loss. For keV H atoms, we identify electronic excitations of the target surface as the dominant mechanism for decoherence, whereas for He atoms this contribution is small. The suppression of electronic excitations owing to the band gap of insulators plays an essential role for preserving quantum coherence and thus for the application of fast atom diffraction as a surface analytical tool.

Recently, diffraction phenomena have been observed for grazing scattering of fast atoms with energies up to some keV from insulator surfaces [1,2]. In those experiments diffraction owing to the periodic array of strings of surface atoms can be resolved. For an angular resolution of typically mrad and spacings between adjacent low indexed strings of some Å, diffraction patterns can be observed for light atoms and molecules up to several keV [1–11].

In addition to insulator surfaces, diffraction patterns were observed for metal [5,6], semiconductor [10] as well as for adsorbates [7,8], and ultrathin oxide films on a metal substrate [11]. For the LiF(001) surface the rumpling, i.e., a relative shift of the two atomic species in the topmost surface layer, was derived with improved accuracy from fast atom diffraction (FAD) [12,13]. The perspectives of FAD as a new surface analytical tool are promising: the extreme sensitivity to the corrugation of the atomic potential in front of the surface, highly efficient detection, negligible damage of the target, and no charging effects. As a possible application of the method we mention organic materials which are fragile to photon or electron bombardment.

Aside from the experimental resolution, the coherence in the collision process plays a key role. Since the interactions of fast atoms with solids have high probabilities for excitations of the target, the observation of quantum scattering for fast atoms was surprising at first glance. Whereas for atom scattering at thermal energies [14] interactions with thermally displaced lattice atoms constitute the main source for decoherence, at higher projectile energies, i.e., keV energies, pronounced electronic excitations of the solid are expected to play a dominant role.

Decoherence is indeed a key issue for this topic [15], since the observed diffraction effects can only be understood by a considerable suppression of such excitation processes. It turns out that specific features for scattering of fast atoms under surface channeling [16], i.e., a steering of projectiles by strings (axial channeling) or planes (planar channeling) of topmost surface atoms in terms of

small-angle scattering [17], are favorable to preserve quantum coherence.

In recent papers, the energy transfer from projectiles to thermally displaced lattice atoms was considered as a dominant source of decoherence for FAD [4,12,18,19]. Since for grazing scattering the energy and momentum transfer to individual target atoms are much smaller than for impact under large angles [20], dephasing for quantum scattering is reduced. In terms of quantum coherence, the Debye-Waller factor becomes sufficiently large for surface channeling in terms of small-angle scattering of projectiles with a major number of target atoms [18,19].

In this Letter we will demonstrate the role of electronic excitations for decoherence by the coincident detection of angular distributions for scattered atoms with their energy loss. We reveal the dominance of different decoherence mechanisms for keV H and He atoms. Our work provides an important basis for a deeper understanding of the nature of quantum scattering and, in particular, of the regime of application of FAD a as surface analytical tool.

So far concerning decoherence for FAD, it was implicitly assumed that electronic excitations of the surface play a negligible role. This was motivated by the wide band gap of the considered LiF(001) surface which gives rise to a substantial suppression of electronic excitations compared to metal targets. However, former studies on grazing scattering of fast atoms from surfaces of ionic crystals with a large band gap have shown that electronic excitations can be efficient [21,22]. As a prominent example we mention high fractions of negative ions for impact of reactive atoms on alkali halide surfaces, accompanied by formation of surface excitons and emission of electrons [23], where efficient capture of electrons from F⁻ sites is mediated by the Madelung potential of the surrounding point charge lattice [24].

In our experiments we have scattered neutral hydrogen and helium atoms with energies from about 100 eV to some keV from a clean and flat LiF(001) surface under a grazing angle of incidence Φ_{in} of about 1°. The target surface was

prepared by cycles of grazing sputtering with 25 keV Ar$^+$ ions and subsequent annealing to about 350 °C. The fast neutral atoms were produced via neutralization of ions in a gas cell in front of a UHV chamber (base pressure some 10^{-11} mbar). In order to measure the energy loss of scattered projectiles, the incident ion beam was chopped by means of electric field plates. Two-dimensional angular distributions of scattered projectiles were recorded at a distance of 96 cm behind the target using of a position sensitive microchannel plate (MCP) detector [25] where the arrival time of a projectile at the MCP served as start for a time-of-flight (TOF) measurement. The position of detected particles and the flight time were stored in a list mode file which allows us to relate angular distributions to specific energy losses for scattered projectiles. Neutral atoms were used, since electron capture and eV energy gain for the motion normal to the surface owing to image charge acceleration [16] already leads to pronounced decoherence.

In Fig. 1(a) we show angular distributions for scattering of 1 keV H atoms from a LiF(001) surface under $\Phi_{\text{in}} = 1.7°$ at room temperature. The incident beam was aligned along the $\langle 110 \rangle$ direction of the surface so that scattering proceeds in the regime of axial surface channeling. The measurements were quite elaborate in order to obtain reasonable statistics, since for the chopped and highly collimated beam the count rates were only some 10 counts per sec. In Fig. 1(b) we present the energy loss spectrum as obtained with our TOF setup. This spectrum reveals the established features of elastically scattered atoms (peak with negligible energy loss) and of discrete energy losses owing to the excitation of surface excitons and emission of electrons, where the energy loss is related to the energies of exciton state and band gap of LiF [21,22].

The angular distribution in Fig. 1(a) shows defined diffraction patterns where positions of peaks are in accord with the Bragg relation $n\lambda_{\text{dB}} = d \sin\Psi$, with n being the diffraction order, Ψ the azimuthal exit angle, d the distance between adjacent strings of equivalent surface atoms, and $\lambda_{\text{dB}} = h/M\nu$ the de Broglie wavelength of the matter wave for a particle of mass M and velocity ν (h is the Planck constant). Note that for 1 keV H atoms, λ_{dB} amounts to 0.009 Å, which is more than 2 orders of magnitude smaller than the width $d = 2.84$ Å of the $\langle 110 \rangle$ channel for LiF(001). For quantum scattering from the surface, the angular widths of diffraction peaks are sufficiently small so that the resulting angular splitting of $\Delta\Psi = 0.18$ deg can be resolved.

A striking result is the coincident link to the energy loss spectrum. Relating the angular distributions to elastically scattered H atoms [prominent peak with negligible energy loss in Fig. 1(b)] results in a distribution widely free from a diffuse background as shown in Fig. 1(d). The background signal can be attributed to scattered projectiles which show an energy loss owing to electronic excitations of the target surface. In Fig. 1(c) we present the angular distribution for atoms with an energy loss around 12 eV owing to excitation of an exciton or emission of an electron. This demonstrates clearly that such inelastic processes attributed to local excitations of the target lead to complete decoherence and to a disappearance of the diffraction pattern. Concerning internal excitations, this points towards the production of well-localized Frenkel excitons [26]. In passing we note that data, as shown in Fig. 1, offer the potential of coherent surface exciton spectroscopy [27,28] with extreme sensitivity to the topmost surface layer.

In similar experiments with 1 keV He atoms (see also below), we observed in the TOF spectrum elastically scattered projectiles only. Then decoherence is dominated by collisions with thermally displaced target atoms [4,18]. The decoherent part of the angular distribution is only slightly broadened compared to the coherent one, so that it is difficult to disentangle both contributions.

In order to disentangle the coherent and incoherent contributions for scattering of H atoms, we analyzed the profile of Bragg peaks in more detail. The incident beam was directed along a high indexed azimuthal direction ("random" orientation). Then scattering proceeds in the regime of planar surface channeling [16,17], and for coherent scattering only the diffraction peak of zeroth order is present. In Fig. 2 we show the azimuthal projection of an angular distribution for 1 keV H atoms scattered from LiF (001) with $\Phi_{\text{in}} = 1.7°$ under random azimuth. Here only a single well-defined diffraction peak of order $n = 0$ appears, superimposed on a broader peak. The diffraction
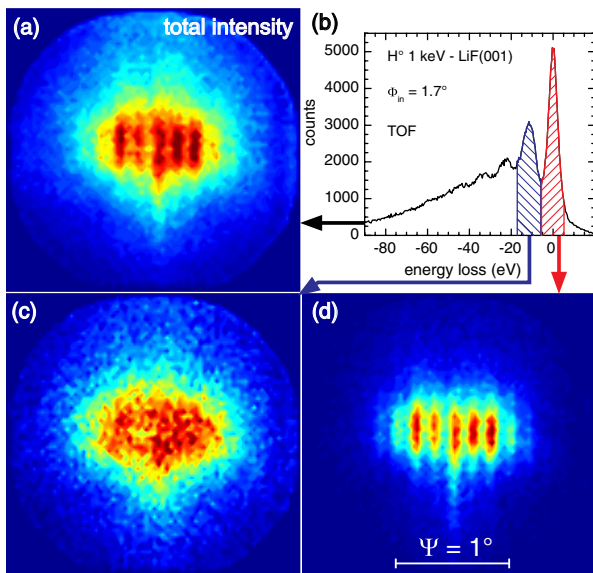

FIG. 1 (color online). Angular distributions recorded with position sensitive detector and energy loss spectrum via TOF for scattering of 1 keV H atoms from LiF(001) under $\Phi_{\text{in}} = 1.7°$ along $\langle 110 \rangle$. (a) Total intensity, (b) energy loss spectrum, (c) intensity coincident with energy loss around 12 eV, (d) intensity coincident with elastic scattering.
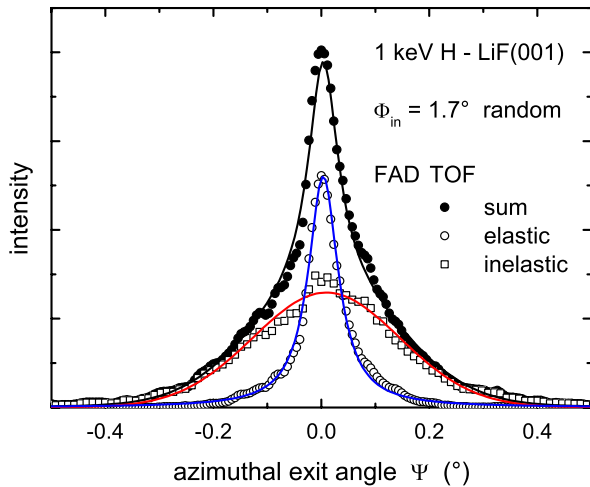
FIG. 2 (color online). Projected intensities as function of azimuthal exit angle for scattering of 1 keV H atoms at $\Phi_{in} = 1.7°$ for random orientation. Full circles, total distribution; open circles, coincident with elastically scattered projectiles; open squares, coincident with energy loss larger than 10 eV. Full curves, fits to Gaussian and Lorentzian line shape and sum of both.

peak has the same angular width as the incident beam of typically 1 mrad ≈ 0.06 deg; i.e., the width of the peak is determined by the divergence for the projectile beam achieved via the collimating slits.

From the projectile energy loss measured in coincidence with the angular distribution, we can relate the narrow peak to elastically scattered H atoms, whereas the broader peak stems from projectiles which show an energy loss larger than about 10 eV owing to electronic excitations of the LiF surface. We thus ascribe the narrow peak to coherent scattering and the broader structure to incoherent classical scattering. Then data as shown in Fig. 2 allow us to obtain information on the degree of decoherence in the scattering process. In former work it was shown that for scattering of H atoms from alkali halide surfaces the electronic excitations depend sensitively on the scattering conditions, i.e., projectile energy and angle of incidence [22,29]. Therefore, we expect that decoherence shows a similar pronounced dependence on these parameters.

In Fig. 3 we show angular distributions for scattering of H atoms from LiF(001) under random azimuthal orientation of the target surface for Φ_{in} ranging from 0.60° to 1.92°. The distributions show a sharp peak superimposed on a broader one which grows with increasing angle. This corresponds to enhanced decoherence in the scattering process. Analysis of the distributions in terms of a pseudo-Voigt line shape (superposition of broad Gaussian and Lorentzian of width as incident beam) provides information on the fractions of coherently (area under Lorentzian) or incoherently (area under Gaussian) scattered atoms.

In Fig. 4 we have plotted the incoherent fractions from the analysis of FAD as shown in Fig. 3, the excitation
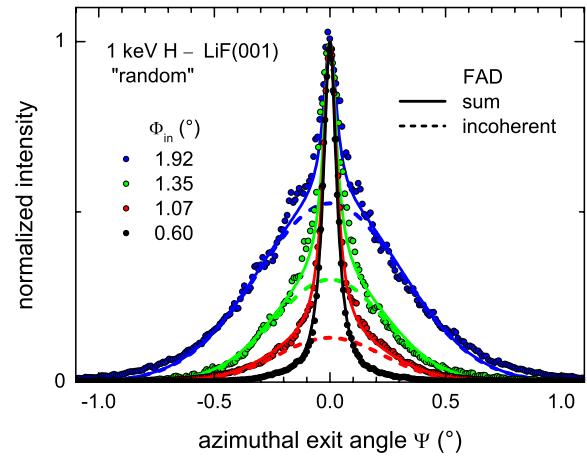

FIG. 3 (color online). Projected intensities as function of azimuthal exit angle for scattering of 1 keV H atoms from LiF(001) under different Φ_{in} for random orientation. Solid curves, fits to experimental distributions; dashed curves, incoherent background.

probabilities from TOF [29], and coincident TOF FAD as shown in Fig. 2 as a function of angle of incidence. These quantities coincide within the scatter of data which demonstrates the close relation of electronic excitations and decoherence. The steep rise with angle is related to enhanced electron capture probabilities at larger angles Φ_{in}. Above about 2° scattering is completely incoherent.

The energy dependence of these fractions for H atoms scattered at $\Phi_{in} = 1.2°$ is shown in Fig. 5. The FAD, TOF, and TOF FAD data match closely. Data shown in Figs. 4 and 5 can be considered as a key feature for the regime of applicability of FAD and its relation to electronic excitations. In order to resolve diffraction patterns, the projectile de Broglie wavelength should be larger than about 0.003 Å, i.e., projectile energies up to some keV. For H atoms, however, electronic excitations set an upper limit for
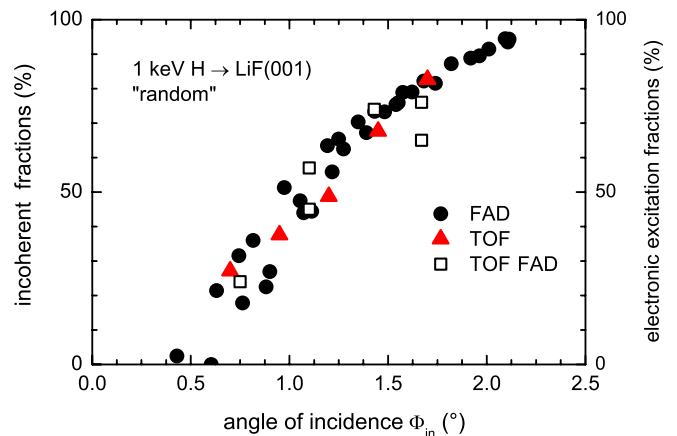

FIG. 4 (color online). Incoherent and electronic excitation fractions as function of angle of incidence for scattering of 1 keV H atoms from LiF(001) for random orientation. Full circles, FAD; red full triangles, TOF; open squares, TOF FAD.
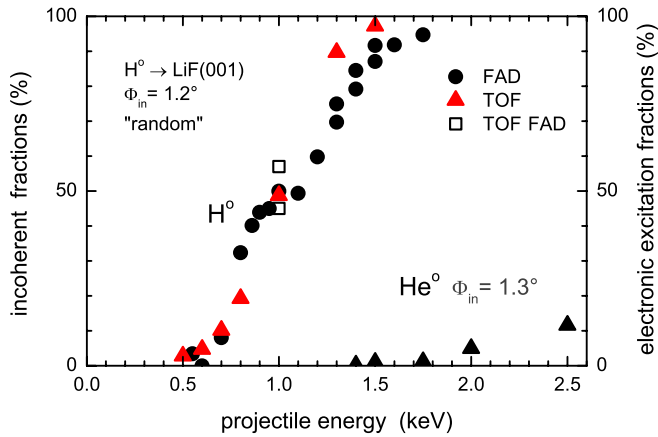
FIG. 5 (color online). Incoherent and electronic excitation fractions as function of projectile energy for scattering of H atoms from LiF(001) under $\Phi_{in} = 1.2°$ (full circles, FAD; red full triangles, TOF; open squares, TOF FAD) and He atoms (TOF) under $\Phi_{in} = 1.3°$ (full triangles) for random orientation.

FAD at around 1 keV. Owing to smaller excitation probabilities for He atoms, most of the coherence is preserved (TOF data for He in Fig. 5). Thus, He atoms for FAD can be used at higher energies and possibly be considered as the best projectile for diffraction studies.

In conclusion, from FAD studies with H atoms based on the coincident detection of angular distributions of scattered atoms and their energy loss, electronic excitations were found as the main source for quantum decoherence. Such local excitations of the surface provide, in principle, information on the path of projectiles and thus destroy quantum interference. At specific conditions, i.e., small angles of incidence and sufficiently small projectile energies, this interaction channel is suppressed so that quantum coherence persists or other sources of decoherence play a role. From a practical point of view, we could clear up the energy range for the application of FAD as a surface analytical tool for wide band gap materials such as alkali halides or oxides.

*Author to whom correspondence should be addressed.
winter@physik.hu-berlin.de

[1] A. Schüller, S. Wethekam, and H. Winter, Phys. Rev. Lett. **98**, 016103 (2007).

[2] P. Rousseau, H. Khemliche, A. G. Borisov, and P. Roncin, Phys. Rev. Lett. **98**, 016104 (2007).

[3] A. Schüller and H. Winter, Phys. Rev. Lett. **100**, 097602 (2008).

[4] P. Rousseau *et al.*, J. Phys. Conf. Ser. **133**, 012013 (2008).

[5] N. Bundaleski, H. Khemliche, P. Soulisse, and P. Roncin, Phys. Rev. Lett. **101**, 177601 (2008).

[6] M. Busch, A. Schüller, S. Wethekam, and H. Winter, Surf. Sci. **603**, L23 (2009).

[7] A. Schüller, M. Busch, S. Wethekam, and H. Winter, Phys. Rev. Lett. **102**, 017602 (2009).

[8] A. Schüller *et al.*, Phys. Rev. B **79**, 235425 (2009).

[9] A. Schüller, H. Winter, M. S. Gravielle, J. M. Pruneda, and J. E. Miraglia, Phys. Rev. A **80**, 062903 (2009).

[10] H. Khemliche, P. Rousseau, P. Roncin, V. H. Etgens, and F. Finocchi, Appl. Phys. Lett. **95**, 151901 (2009).

[11] J. Seifert, A. Schüller, H. Winter, R. Wlodarczyk, J. Sauer, and M. Sierka, Phys. Rev. B **82**, 035436 (2010).

[12] F. Aigner, N. Simonović, B. Solleder, L. Wirtz, and J. Burgdörfer, Phys. Rev. Lett. **101**, 253201 (2008).

[13] A. Schüller *et al.*, Phys. Rev. A **82**, 062902 (2010).

[14] D. Farías and K.-H. Rieder, Rep. Prog. Phys. **61**, 1575 (1998).

[15] W. H. Zurek, Rev. Mod. Phys. **75**, 715 (2003).

[16] H. Winter, Phys. Rep. **367**, 387 (2002).

[17] D. Gemmell, Rev. Mod. Phys. **46**, 129 (1974).

[18] J. R. Manson, H. Khemliche, and P. Roncin, Phys. Rev. B **78**, 155408 (2008).

[19] A. C. Levi, J. Phys. Condens. Matter **21**, 405004 (2009).

[20] A. Mertens and H. Winter, Phys. Rev. Lett. **85**, 2825 (2000).

[21] P. Roncin, J. Villette, J. P. Atanas, and H. Khemliche, Phys. Rev. Lett. **83**, 864 (1999).

[22] H. Winter, in *Correlation Spectroscopy of Surfaces, Thin Films, and Nanostructures*, edited by J. Berakdar and J. Kirschner (Wiley, Weinheim, 2004), p. 151.

[23] C. Auth, A. G. Borisov, and H. Winter, Phys. Rev. Lett. **75**, 2292 (1995).

[24] A. G. Borisov, V. Sidis, and H. Winter, Phys. Rev. Lett. **77**, 1893 (1996).

[25] DLD40, Roentdek Handels GmbH, http://www.roentdek.de

[26] P. Abbamonte *et al.*, Proc. Natl. Acad. Sci. U.S.A. **105**, 12 159 (2008).

[27] G. D. Scholes, Nature (London) **466**, 1047 (2010).

[28] D. B. Turner and K. A. Nelson, Nature (London) **466**, 1089 (2010).

[29] S. Lederer *et al.*, Nucl. Instrum. Methods Phys. Res., Sect. B **203**, 23 (2003).